

Effect of Orbital Rotation and Mixing on the Optical Properties of Orthorhombic $RMnO_3$ ($R = La, Pr, Nd, Gd, \text{ and } Tb$)

M. W. Kim,¹ S. J. Moon,¹ J. H. Jung,² Jaejun Yu,³ Sachin Parashar,¹ P. Murugavel,¹ J. H. Lee,¹ and T. W. Noh^{1,*}

¹ReCOE & School of Physics, Seoul National University, Seoul 151-747, Korea

²Department of Physics, Inha University, Incheon 402-751, Korea

³CSCMR & School of Physics, Seoul National University, Seoul 151-747, Korea

(Received 7 April 2005; published 20 June 2006)

We investigated the ab -plane absorption spectra of $RMnO_3$ ($R = La, Pr, Nd, Gd, \text{ and } Tb$) thin films. As the ionic radius of the R ion decreases, we observed a drastic suppression of the 2 eV peak, i.e., the intersite optical transition between spin- and orbital-aligned states across the Mott gap. We found that, in addition to orbital rotation, orbital mixing in the orbital-ordered state should play an important role in the suppression of 2 eV peak. We also found that the spectral weight of 2 eV peak is proportional to the A -type antiferromagnetic ordering temperature, which suggests that the magnetic interaction should be sensitively coupled to the orbital degree of freedom.

DOI: 10.1103/PhysRevLett.96.247205

PACS numbers: 75.70.-i, 77.90.+k, 78.20.-e

$LaMnO_3$ has been known as a parent compound of the colossal magnetoresistance manganites, where charge, spin, lattice, and orbital degrees of freedom interplay with each other [1]. $LaMnO_3$ has an orthorhombic structure with four $3d$ electrons: three t_{2g} and one e_g electrons. Since three t_{2g} electrons form an orbitally closed shell, many physical properties are believed to be determined by its e_g electron. In its ground state, $LaMnO_3$ is a Mott insulator [2–4] with the A -type spin and the C -type orbital orderings, as schematically drawn in Figs. 1(a) and 1(b), respectively. The antiferromagnetic (AFM) ordering temperature T_N is about 140 K, and the orbital ordering temperature is around 800 K. The occurrence of the spin- and orbital-ordered state has been understood in terms of the cooperative Jahn-Teller distortion [5].

Rare-earth substitutions of the La ion provide an intriguing phase diagram for $RMnO_3$ [6], as illustrated in Fig. 1(c). As the ionic radius (r_R) of the R ion decreases, the crystal structure of $RMnO_3$ changes from orthorhombic ($R = La - Dy$) to hexagonal ($R = Ho - Lu$). $TbMnO_3$ and $DyMnO_3$ are located near the structural phase boundary, and they have attracted lots of attention recently due to their complicated low temperature magnetic states and multiferroic properties [6,7]. On the other hand, the magnetic properties of the orthorhombic perovskite $RMnO_3$ ($R = La - Tb$) has a rather simple R dependence: T_N decreases with decreasing r_R . Structural deformations, such as buckling and distortion of the MnO_6 octahedra, also increase. According to the Goodenough-Kanamori rule [5,8], the orbital overlap of electrons should be crucial in determining the magnetic interaction. The rule takes into account only the overlap in terms of the Mn-O-Mn bond angle ϕ . However, the rapid decrease of T_N with the R -ion substitution is rather unexpected, since the change of ϕ is less than 10° . Therefore, reinvestigation on the orbital overlap in $RMnO_3$ ($R = La - Tb$) could provide us further insights to understand their intriguing physical properties.

Optical spectroscopy has been known to be a powerful tool to investigate the orbital degrees of freedom, especially the orbital correlation between neighboring sites [2,3,9,10]. In this Letter, we report the ab -plane optical responses of epitaxial $RMnO_3$ ($R = La, Pr, Nd, Gd, \text{ and } Tb$) films. As r_R decreases, the spectral weight of the intersite transition across the Mott gap, located around

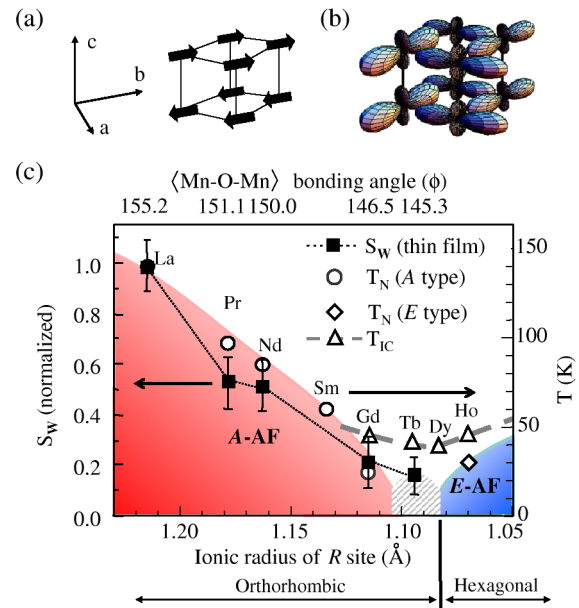


FIG. 1 (color online). (a) The A -type spin and (b) the C -type orbital ordering pattern of electrons at the Mn sites in $LaMnO_3$. (c) A schematic magnetic phase diagram of $RMnO_3$, redrawn from Ref. [6]. The spectral weight of 2 eV peak, S_W (solid square), shows similar r_R dependence with the A -type AFM ordering T_N (open circles). The E -type AFM ordering T_N (open diamond) and the incommensurate spin ordering T_{IC} (open triangles) are also shown. The hatched area represents the region where the commensurate spin order and ferroelectric property emerges.

2 eV, decreases rapidly. This dramatic reduction of the spectral weight cannot be explained in terms of the ϕ change only. We demonstrate that the orbital mixing between two orthogonal e_g orbitals should also play an important role in the spectral weight change.

High quality $RMnO_3$ ($R = \text{La, Pr, Nd, Gd, and Tb}$) thin films were grown on double-side-polished $(\text{LaAlO}_3)_{0.3}(\text{SrAl}_{0.5}\text{Ta}_{0.5}\text{O}_3)_{0.7}$ substrates by a pulsed laser deposition technique. From x-ray diffraction (XRD) measurements, it was found that all the films were grown epitaxially with their c axis perpendicular to the film surfaces. The c -axis lattice constants in pseudocubic lattice for the LaMnO_3 , GdMnO_3 , and TbMnO_3 films were found to be about 3.94 Å, 3.73 Å, and 3.71 Å, respectively, close to the single crystal values. The c -axis lattice constants for the other films were difficult to be determined, since their XRD peaks are too close to substrate peaks. Cross-sectional scanning electron microscopy pictures showed that our films were about 400 nm thick. Transmission spectra of the films were measured from 0.4 to 4.0 eV by a grating spectrophotometer. The absorption coefficients were determined by taking the logarithm of the transmittance, subtracting that of the substrate, and dividing by the film thickness. Since the normal-incident optical geometry was used, the absorption spectra should come from the ab -plane responses of the films.

Figure 2(a) shows the absorption coefficient spectra $\alpha(\omega)$ of $RMnO_3$ at room temperature, where all the samples should be in the C -type orbital-ordered state. The spectra of LaMnO_3 are composed of a peak near 2 eV and stronger absorption peaks above 3 eV. The higher energy absorption features come from the charge transfer transition from O $2p$ to Mn $3d$ [2,9]. The origin of the 2 eV peak has been debated for a long time [2]. Recently, however, it has been shown quite convincingly that the 2 eV peak should be interpreted as an intersite transition across the Mott gap [2,3]. As shown in Figs. 1(a) and 1(b), the correlation-induced transition within the ab plane should occur between e_g orbital states at neighboring sites in the ferromagnetic-spin (FM) and antiferro-orbital (AFO) configuration [11].

Note that the absorption spectra of other $RMnO_3$ have similar spectral features: namely, the 2 eV peak and the strong charge transfer transition above 3 eV. However, as r_R decreases, $\alpha(\omega)$ for the correlation-induced 2 eV peak becomes strongly suppressed. To obtain more quantitative information, we estimated the spectral weight S_W of the 2 eV peak. We first subtracted the charge transfer transition contribution by fitting with linear lines and integrated the remnant spectral weight from 0.4 to 2.7 eV [12]. The experimentally determined S_W , marked as the solid squares in Fig. 2(b), becomes drastically suppressed with decreasing r_R . Such a dramatic decrease of S_W is rather unexpected. All the $RMnO_3$ compounds, studied in this work, have the same orthorhombic crystal structure and the same

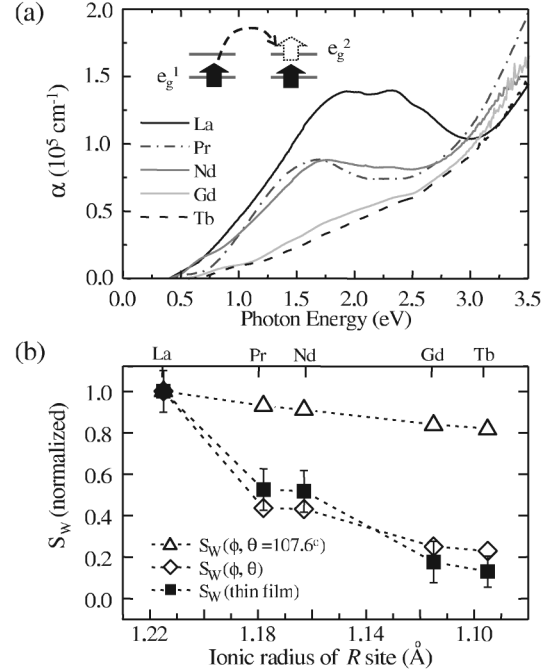


FIG. 2. (a) Absorption spectra of $RMnO_3$ ($R = \text{La, Pr, Nd, Gd, and Tb}$) thin films at room T . The inset schematically represents the intersite transition corresponding to the 2 eV peak. (b) The experimental S_W (solid squares) is compared with the calculation for various ϕ by using the orbitals of LaMnO_3 , i.e., at a fixed θ ($=107.6^\circ$) (open triangles), and for experimental values of ϕ and θ (open diamonds) [15].

spin or orbital ordering pattern, but only with a relatively small variation of ϕ , less than 10° . Therefore, the large suppression of S_W is difficult to be explained only in terms of the ϕ change.

To elucidate the origin of the 2 eV peak suppression, we estimated $\alpha(\omega)$ starting from the Fermi's golden rule:

$$\alpha(\omega) = \frac{2\pi}{\hbar} \sum_f |\langle \psi_f | P | \psi_i \rangle|^2 \delta(\omega - \Delta E_{f-i}), \quad (1)$$

where ΔE_{f-i} is the excitation energy from the initial to the final states. For the 2 eV peak, the initial state ($|\psi_i\rangle$) corresponds to the occupied e_g orbital at one Mn site and the final state ($|\psi_f\rangle$) corresponds to the unoccupied e_g orbital at the neighboring Mn site, shown in the inset of Fig. 2(a). Within the electric dipole approximation [13], S_W will be linearly proportional to $|\langle \psi_f | \nabla | \psi_i \rangle|^2$. This matrix element can be estimated by the second order perturbation process, through the oxygen p orbitals:

$$S_W \propto |\langle \psi_f | \nabla | \psi_i \rangle|^2 \sim \left| \sum_{\alpha} \langle \psi_f | p_{\alpha} \rangle \langle p_{\alpha} | \psi_i \rangle \right|^2 / \Delta, \quad (2)$$

by assuming that the intermediate state energy Δ remains almost unchanged [14]. $|p_{\alpha}\rangle$ ($\alpha = x, y, z$) represents the oxygen p orbitals. As the p orbitals are fully occupied, the $\sum_{\alpha} \langle \psi_f | p_{\alpha} \rangle \langle p_{\alpha} | \psi_i \rangle$ term becomes dependent on the rela-

tive orientation of the Mn e_g orbitals. Since the R -ion substitution causes the buckling and Jahn-Teller distortion of the Mn-O octahedra, we will investigate the roles of these lattice deformations on the R -ion dependent change of S_W .

First, let us consider the contribution of the Mn-O-Mn bond angle (ϕ) change, originated from the buckling. As shown in Fig. 3(a), the buckling of the MnO₆ octahedra in the GdFeO₃ type lattice will cause a decrease in ϕ . Without the buckling (i.e., $\phi = 180^\circ$), the larger lobe of the $|3x^2 - r^2\rangle$ -type orbital of a Mn³⁺ site is aligned to face the smaller lobe of the neighboring orbital, as shown in Fig. 1(b). As the buckling is turned on, the orbital lobe of an electron at one site will rotate with respect to that at the neighboring site, which will result in a reduction in the intersite hopping amplitude and thereby a decrease in S_W . To evaluate the changes in $|\psi_i\rangle$ and $|\psi_f\rangle$ quantitatively, the rotation of the orbitals in the ab plane was formulated in terms of the rotational transformation of the local (x_2, y_2) coordinates by ϕ relative to the local (x_1, y_1) coordinates, as shown in Fig. 3(a). Here, the local z_1 and z_2 axis directions are assumed to be the same. When the orbital wave functions of LaMnO₃ were used, it was found that the orbital rotation effect on S_W is proportional to $\cos^2\phi$. As shown in Fig. 1(c), the R -ion substitution in $RMnO_3$ makes ϕ vary from 155.2° to 145.3° [15]. In Fig. 2(b), the calculated values of S_W are plotted with the open triangles. It is obvious that the variation in ϕ alone cannot account for the large change in the experimental S_W .

In a undistorted MnO₆ octahedron, two e_g orbitals remain doubly degenerate. Under the Jahn-Teller distortion along the z direction, the e_g orbitals become split into two orthogonal orbitals, i.e., $|3z^2 - r^2\rangle$ and $|x^2 - y^2\rangle$. However, using neutron scattering measurements, Alonso *et al.* showed that the actual occupied e_g orbital of $RMnO_3$ should be a mixed state of $|3z^2 - r^2\rangle$ and $|x^2 - y^2\rangle$ orbitals due to the local distortion of the MnO₆ octahedron [15]. In addition, they experimentally reported the degrees of the orbital mixing for $RMnO_3$ [15].

Now, by including the orbital mixing effects, we can reexamine the R -ion dependent S_W change. For a quantitative analysis using Eq. (2), we constructed the realistic Mn e_g orbitals using the orbital mixing angle θ : the occupied orbital at the site 1 and the unoccupied orbital at the neighboring site 2 are written as

$$\begin{aligned} |\psi_1^{\text{occ}}\rangle &= \cos\frac{\theta}{2}|3z_1^2 - r_1^2\rangle + \sin\frac{\theta}{2}|x_1^2 - y_1^2\rangle, \\ |\psi_2^{\text{unocc}}\rangle &= -\sin\frac{\theta}{2}|3z_2^2 - r_2^2\rangle + \cos\frac{\theta}{2}|x_2^2 - y_2^2\rangle, \end{aligned} \quad (3)$$

where the subscripts in the wave functions represent the different local coordinates. The unoccupied orbital, corresponding to the final state of the transition, is orthogonal to the occupied orbital at site 2. To visualize the orbital mixing effects, the occupied orbitals for three different θ

values are plotted in Fig. 3(b). [Note that the orbital configuration shown in Fig. 1(b) corresponds to $\phi = 180^\circ$, $\theta = 107.6^\circ$.] From Eqs. (2) and (3), we obtain,

$$S_W \propto \left\{ \left(\sin\theta - \frac{\sqrt{3}}{2} \right) \cos\phi \right\}^2. \quad (4)$$

Using the reported (θ, ϕ) values from the neutron scattering experiment [15], we can estimate the values of $S_W(\theta, \phi)$ and plot them with the open diamonds in Fig. 2(b). The theoretical $S_W(\theta, \phi)$ values agree quite well with the experimental S_W change. It clearly demonstrates that both orbital rotation and mixing are responsible for the observed drastic suppression of S_W .

The θ and ϕ dependence of S_W is displayed in Fig. 3(c). Note that $\theta = 107.6^\circ$ for LaMnO₃ and $\theta = 114.3^\circ$ for TbMnO₃. Although the variation of the θ value is about 6.7° , smaller than that of the ϕ value (i.e., about 9.9°), the variation of S_W due to the orbital mixing change is larger than that due to the ϕ change. A possible reason is the strong anisotropy in the shape of the orbitals. When $\theta = 90^\circ$, the occupied and unoccupied orbitals given in Eq. (3) have the mean state of the two orthogonal orbitals. As θ increases, the $|x^2 - y^2\rangle$ orbital enhances the wave function overlap and the $|3z^2 - r^2\rangle$ orbital reduces it within the ab plane, so the mixing of those two orbitals results in the

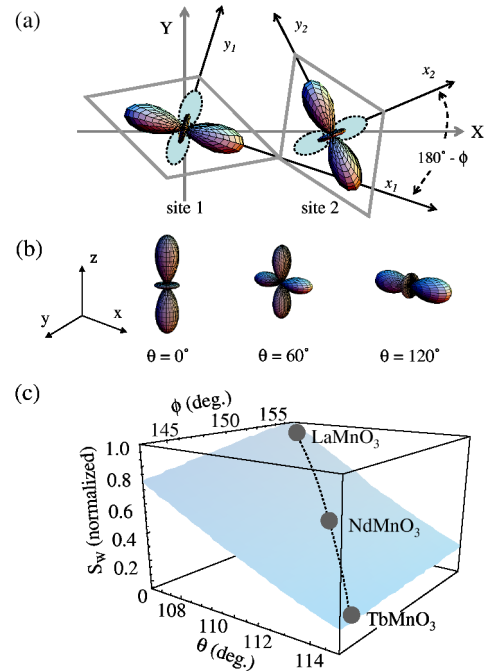


FIG. 3 (color online). The setup is schematically shown for the calculation of the orbital mixing angle (θ) and the Mn-O-Mn bond angle (ϕ) dependent S_W . (a) The local coordinates (x, y) for the MnO₆ octahedra and the Mn e_g orbitals. (The orbital lobes drawn with the dashed lines schematically represent the unoccupied orbitals.) (b) The occupied orbitals of selected θ values. (c) The calculated S_W as a function of θ and ϕ .

minimum around $\theta = 120^\circ$ in Eq. (4). As shown in Fig. 3(c), $RMnO_3$ are located near the (θ, ϕ) region where S_W will change rapidly and depend strongly on θ . Thus, the orbital mixing becomes a crucial factor in numerous physical properties of $RMnO_3$, which has been rarely noticed before.

The S_W values for various $RMnO_3$ are marked with the solid squares in Fig. 1(c). It is remarkable to note that the r_R dependence of the S_W change is quite similar to that of T_N , i.e., the A -type AFM ordering temperature. With decreasing r_R from La to Tb, T_N decreases systematically, i.e., from ~ 140 K for $LaMnO_3$ to nearly zero for $TbMnO_3$. Similarly, S_W also becomes significantly reduced. These similar R dependencies of S_W and T_N are rather surprising, since the S_W change comes from the ab -plane response while the AFM ordering at T_N occurs along the c axis.

One possible explanation for this intriguing phenomenon could be an occurrence of additional FM component in the interplane interactions along the c axis due to the buckling of the MnO_6 octahedra. In the undistorted case (i.e., $\phi = 180^\circ$), the A -type spin order is attributed to the FM e_g - e_g interaction within the ab plane and the AFM t_{2g} - t_{2g} superexchange interaction along the c axis. Here T_N is mainly determined by the latter, since it is much weaker than the ab -plane FM interaction [16]. When the buckling of the MnO_6 octahedra occurs; however, the overlap of the e_g orbitals between the Mn planes brings out a new FM interaction along the c axis. Although T_N of $RMnO_3$ will be determined as a result of the competition between the AFM and the FM interactions, the r_R dependence of T_N seems to be more sensitive to the latter. The FM interaction should critically depend on the buckling, while the AFM superexchange interaction remains insensitive to the structural change due to the inert nature of the closed shell t_{2g} orbitals. Since the FM interaction does arise from the tilting of the MnO_6 octahedra, the interaction could be closely related to S_W , which is proportional to the square of the electron hopping matrix in the ab plane. This scenario suggests that the AFM and FM interactions will compete with each other and achieve a balance around $TbMnO_3$. Our picture based on a new FM interaction along the c axis could provide a new starting point to explain the intriguing magnetic states near the multiferroic phases.

The original Goodenough-Kanamori rule takes account of the orbital overlap only in terms of ϕ [5,8]. Then, the sign of the effective magnetic interactions (i.e., AFM and FM ground states) is expected to change near $\phi = 135^\circ$. In $RMnO_3$, the $GdFeO_3$ type distortion can induce the competition between AFM and FM along the c axis, so one could envisage the disappearance of AFM near 135° . However, as displayed in Fig. 1(c), the A -type AFM order in the orthorhombic $RMnO_3$ disappears at $\phi \gtrsim 145^\circ$. This

work shows that the Goodenough-Kanamori rule should remain to be valid when the additional contribution of the orbital mixing to the orbital overlap is properly considered.

In summary, we reported the drastic change of the 2 eV peak spectral weight of $RMnO_3$ ($R = La, Pr, Nd, Gd,$ and Tb) with rare-earth-metal ion substitution. The spectral weight change was successfully understood in terms of the optical matrix element when the rotation and the mixing of the orbital were taken into account. The close correlation between the 2 eV spectral weight and the A -type antiferromagnetic ordering temperature suggests that the superexchange interaction in $RMnO_3$ could be tuned by the orbital degree of freedom.

We acknowledge valuable discussions with J.S. Lee, K.W. Kim, S.S.A. Seo, K.H. Ahn, P. Littlewood, P. Horsch, J.A. Alonso, and J.B. Goodenough. This work was supported by the KOSEF CRI program and CSCMR SRC, and also supported by the Korean Ministry of Education BK21 project.

Note added.—Recently, we found that similar optical measurements had been done on single crystalline $RMnO_3$ samples [17]. We estimated the S_W of the 2 eV peak from the single crystal data, and found that they show nearly the same r_R dependence with the S_W data of our thin films.

*Corresponding author.

Email address: twnoh@phya.snu.ac.kr

- [1] Y. Tokura and N. Nagaosa, *Science* **288**, 462 (2000).
- [2] M. W. Kim *et al.*, *New J. Phys.* **6**, 156 (2004).
- [3] N. N. Kovaleva *et al.*, *Phys. Rev. Lett.* **93**, 147204 (2004).
- [4] T. Inami *et al.*, *Phys. Rev. B* **67**, 045108 (2003).
- [5] J. B. Goodenough, *Phys. Rev.* **100**, 564 (1955).
- [6] T. Kimura *et al.*, *Phys. Rev. B* **68**, 060403(R) (2003).
- [7] T. Kimura *et al.*, *Nature (London)* **426**, 55 (2003).
- [8] J. Kanamori, *J. Phys. Chem. Solids* **10**, 87 (1959).
- [9] M. W. Kim *et al.*, *Phys. Rev. Lett.* **89**, 016403 (2002), and references therein.
- [10] M. W. Kim *et al.*, *Phys. Rev. Lett.* **92**, 027202 (2004).
- [11] Recent resonant x-ray scattering measurements also support this assignment. See Ref. [4].
- [12] We also fitted the 2 eV peak and the charge transfer transitions with the Lorentz oscillators and subtracted the latter contribution. Even with this different fitting, the r_R dependence of S_W [Fig. 2(b)] remains almost the same.
- [13] L. C. Lew Yan Voon and L. R. Ram-Mohan, *Phys. Rev. B* **47**, 15 500 (1993).
- [14] P. W. Anderson, in *Magnetism I*, edited by G. T. Rado and H. Suhl (Academic, New York, 1963).
- [15] J. A. Alonso *et al.*, *Inorg. Chem.* **39**, 917 (2000).
- [16] K. Hirota *et al.*, *J. Phys. Soc. Jpn.* **65**, 3736 (1996).
- [17] K. Tobe, Ph.D. thesis, University of Tokyo, 2003.